Magnetically and Optically Tunable Terahertz Radiation from Ta/NiFe/Pt Spintronic Nanolayers Generated by Femtosecond Laser Pulses

R. Adam,[1] G. Chen,[2] D. E. Bürgler,[1] T. Shou,[3] I. Komissarov,[3] S. Heidtfeld,[1] H. Hardtdegen,[4] M. Mikulics,[1] C. M. Schneider,[1,5] and R. Sobolewski[2,3]

[1]Research Centre Jülich, Peter Grünberg Institute
[2]Materials Science Graduate Program and Laboratory for Laser Energetics, University of Rochester
[3]Department of Electrical and Computer Engineering and Laboratory for Laser Energetics, University of Rochester
[4]Research Centre Jülich, Ernst Ruska Centre for Microscopy and Spectroscopy with Electrons
[5]Department of Physics, University of California, Davis

Terahertz (THz) radiation covers the electromagnetic spectrum range between radiofrequency millimeter waves and optical far-infrared radiation, approximately 0.3 to 30 THz, and has been applied in astronomy, medical imaging, security, communication, and manufacturing[1,2] as well as a scientific tool in materials testing[3] and bio imaging,[4] or in the study of electron wakefield acceleration.[5] Among different THz sources, current extensive research focuses on emitters of ultrafast electromagnetic transients with a broad THz-range spectrum in order to control and capture spin,[6] charge,[7] or phase-transition–related processes on subpicosecond time scales. Recent observation of THz emissions from optically excited ferromagnet/metal (F/M) nanolayers[8–11] establishes a very elegant link between laser optics, spintronics, and THz radiation, merging these three very active scientific fields and having a tremendous potential for future applications. The uncomplicated fabrication of spintronic THz emitters can lead to widespread applications.

Superdiffusive spin currents generated in laser-driven demagnetization experiments have been theoretically predicted[12] and, subsequently, quickly confirmed in a number of experiments,[13–17] demonstrating their crucial role in ultrafast magnetization dynamics in a range of magnetic materials and structures. The central role of the superdiffusive currents in THz generation[9] has further strengthened their importance in laser-driven spin transient dynamics and has led to applications that are currently emerging at the border of laser physics and spin-based electronics. A simple physical mechanism has been proposed to explain the generation of THz transients from femtosecond laser-driven F/M bilayers and multilayers. THz emission is explained by the photon-driven spin current flowing from an F film to a neighboring M material. This spin current is, subsequently, converted by the inverse spin Hall effect (ISHE) into a transient charge current flowing along the M surface, thereby generating a laser-helicity independent subpicosecond electromagnetic signal.[10,18]

We have generated bursts of strong THz radiation (transient, single-picosecond-in-duration electromagnetic signals) by placing Ta/NiFe/Pt (equivalently, Ta/Py/Pt, where Py stands for permalloy: $Ni_{80}Fe_{20}$) trilayers in a static magnetic field and illuminating them with a train of 100-fs-wide laser pulses from a commercial Ti:sapphire laser (800-nm wavelength and 76-MHz repetition rate). The train of laser pulses was split into two beams with a 90:10 intensity ratio. The high-intensity branch, after bouncing from a retroreflector mounted at the delay stage, was focused at our F/M sample, while the low-intensity beam was used to excite a photoconductive low-temperature–grown GaAs (LT-GaAs) switch acting as a THz transient detector.[19] The linear motion of the delay stage in the pump beam, with a 2.5-μm-step size, allowed an optical path control with a 16.6-fs time resolution. Ta/Py/Pt samples were optically excited either by illumination of the metallic surface (direct geometry) or by laser pulses passing through the MgO substrate (reverse geometry). In addition, we used a Teflon (polytetrafluoroethylene) lens with a 5-mm diameter and 10-mm focal length to focus the THz radiation at the LT-GaAs detector operated in a photoconductive-sampling mode. The latter allowed us to reconstruct the THz transient in time domain. The external **H** field was generated either by electromagnet

coils wrapped around iron yokes and supplying a variable field of up to 70 kA/m or by a pair of permanent magnets generating a fixed, ~40-kA/m field.

Our spintronic samples consisted of Ta (2-nm)/Py (2-nm)/Pt (2-nm) nanotrilayers and were deposited sequentially at room temperature by magnetron sputtering on top of optically polished 10 × 10-mm^2 MgO substrates with (100) surface orientation. The deposition thickness for each layer was monitored by a quartz crystal microbalance. The thin, 2-nm Ta buffer layer was deposited first, directly onto the MgO substrate to achieve a good adhesion and smoothness of the consecutive layers. We have chosen Pt as a top material for its relatively high spin-orbit coupling: the material-dependent parameter that, according to literature, is responsible for THz generation in magnetic nanolayers.[20]

Figure 1(a) presents a typical time-domain, subpicosecond (0.9-ps FWHM of the main peak) electromagnetic transient generated by our spintronic nanolayer emitter and detected by the LT-GaAs detector. The zero time on the time axis was chosen arbitrarily, but it was kept the same for all measurements. The measurement was done in the reverse geometry, illustrated in the left inset in Fig. 1(a) with the **H** field fixed at 55 kA/m and applied in the sample plane. The laser fluence was 7.25 μJ/cm^2. In this geometry, we have also observed (not shown here) a secondary, significantly weaker THz transient, delayed by ~10 ps with respect to the main signal. The latter signal was identified as a THz transient generated at the Py/Pt bilayer and propagating in the opposite direction with respect to the main one and, subsequently, reflected at the MgO/air interface. A fast Fourier transform (FFT) of the time-domain waveform is shown in the right inset in Fig. 1(a) as the normalized THz transient power spectrum. We note that the signal frequency content extends up to 5 THz with a 3-dB cutoff at 0.85 THz. A small dip visible in the power spectrum at about 2 THz corresponds to resonant absorption of a Teflon lens used to focus the THz beam. When we flipped the trilayer by 180° and illuminated it in the direct geometry, keeping the laser beam and **H** orientation unchanged, we recorded essentially the same time-domain transient as shown in the main panel of Fig. 1(a), but with the polarity reversed. As we discuss below, the latter indicates a reversed direction of the charge current density $\mathbf{J}_C$. Compared to the reverse geometry, the signal in direct geometry had a slightly lower amplitude (apparently caused by THz absorption by Ta and MgO) and no secondary reflected signal was

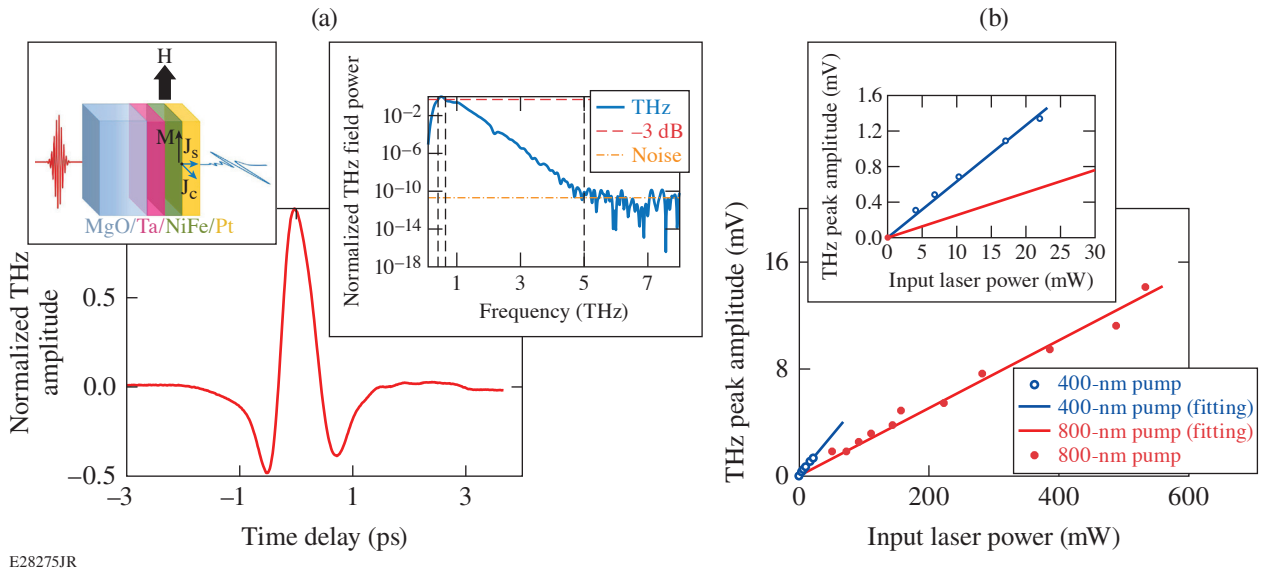

Figure 1
(a) A normalized THz transient generated by a 100-fs-wide laser pulse impinging at a Ta/Py/Pt nanotrilayer through the MgO substrate (reverse illumination geometry). The left inset shows the trilayer stacking and the schematics of the THz-generation mechanism. The right inset presents a normalized THz power spectrum that corresponds to the pulse shown in the main panel. The spectrum exhibits a 3-dB cutoff at 0.85 THz and extends to 5 THz with exponentially decreasing intensity. (b) A THz transient amplitude as a function of the incident laser beam power for both fundamental (λ = 800 nm; solid red circles) and frequency-doubled light (λ = 400 nm; open blue circles). The inset shows the available power range for the 400-nm light and demonstrates a strongly increased efficiency of THz generation at the 400-nm wavelength.

observed. Finally, we optically illuminated the Pt/Py/Ta trilayer from the Pt side at a 45° incidence angle and collected a THz transient with the detector positioned at 90° with respect to the laser beam. As expected for superdiffusive current flowing in all directions, the recorded time-domain waveform had a shape identical to the pulse shown in the main panel of Fig. 1(a). The power spectra for the direct, reverse, and 45° illumination geometries were identical to that presented in Fig. 1(a), right inset. The above observations indicate that optically triggered THz transients originate near or at the Py/Pt interface.

We have also studied the impact of varying external optical excitation on the THz signal emitted by our spintronic Ta/Py/Pt emitter. Figure 1(b) shows the maximum THz-signal amplitude A^{THz} dependence on the incident, average laser power at both the fundamental (λ = 800 nm; solid red circles) and frequency-doubled (λ = 400 nm; open blue circles) wavelengths at a constant magnetic field H = 55 kA/m. In both cases, the dependence is linear, as indicated by the corresponding linear fits. Although the range of available incident powers for the 400-nm light was quite small, limited by the efficiency of the frequency-doubling barium borate (BBO) crystal, our data clearly demonstrate that for the same laser power, 400-nm photons generate approximately 3× larger subpicosecond transients, as compared to the 800-nm photons. At the same time, the corresponding normalized time-domain waveforms (not shown) were practically the same as the one shown in Fig. 1(a), main panel, resulting in the identical THz power spectra. Although our studies seem to contradict recent results of Herapath *et al.*,[21] where no pump wavelength dependence on THz generation was reported, we stress that the measurements presented in Ref. 21 were performed not only on a different material system, but, first of all, exclusively at infrared wavelengths (900 to 1500 nm). High-energy green photons used in our studies are certainly more efficiently absorbed by metallic nanolayers and generate a significantly larger concentration of hot electrons that couple to the spins. As a result, we observe the THz amplitude enhancement as it was discussed above and presented in Fig. 1(b).

An external electromagnet in our THz setup allowed us to tune the **H** field in a range up to ±70 kA/m. For a constant laser light (λ = 800 nm) with an average laser power of 550 mW, we stepped **H** from –70 kA/m to +70 kA/m and back to –70 kA/m, and by this sequence we recorded the A^{THz} dependence on the magnitude of the in-plane **H** field applied to our Ta/Py/Pt trilayer. We observed that the $A^{\mathrm{THz}}(\mathbf{H})$ hysteresis overlaid perfectly on the shape of the static hysteresis of the magnetic moment $\mu(\mathbf{H})$ of the Py nanolayer, recorded using a commercial physical property measurement system (PPMS). Most interestingly, the measured $A^{\mathrm{THz}}(\mathbf{H})$ curve exhibited hysteresis that was significantly narrower than that of the pure Py layer.

The main question is why $A^{\mathrm{THz}}(\mathbf{H})$ for our samples follows the shape of the static hysteresis of the Py film. Our optical beam is linearly polarized, so we are in the laser-helicity independent case and the THz transient is directly proportional to $\mathbf{J}_C$ produced by the ISHE mechanism that in turn depends on the spin current density $\mathbf{J}_S$ and spin polarization $\boldsymbol{\sigma}$. According to, e.g., Saitoh *et al.*[22] $\mathbf{J}_C = D_{\mathrm{ISHE}}(\mathbf{J}_S \times \boldsymbol{\sigma})$, where D_{ISHE} is a coefficient representing the ISHE efficiency in a material. Therefore, we can control the ultrafast time-domain signal amplitude and polarity by controlling the $\mathbf{J}_C$ amplitude and its direction. The $\mathbf{J}_C$ amplitude is controlled in our case through $\boldsymbol{\sigma} \sim \mu(\mathbf{H})$, while the $\mathbf{J}_C$ direction is controlled by the illumination geometry (direct or reverse). We note that in both geometries the superdiffusive current flows in all directions as confirmed by the experiment with laser illumination under 45° mentioned above; nevertheless, only the $\mathbf{J}_C$ component pointing from Py to Pt matters for THz generation. For fixed directions of **H** and $\mathbf{J}_S$, and because $\mathbf{J}_C \sim \mu(\mathbf{H})$, one should expect that $A^{\mathrm{THz}}(\mathbf{H})$ behaves similar/identical to the $\mu(\mathbf{H})$ dependence, as, indeed, is observed in our studies. The observed significantly narrower width of the $A^{\mathrm{THz}}(\mathbf{H})$ hysteresis in the Ta/Py/Pt trilayer as compared to the $\mu(\mathbf{H})$ hysteretic dependence may arise from the fact that the static $\mu(\mathbf{H})$, measured in PPMS, represents a signal averaged over the whole sample volume. Therefore, for instance, pinning at the sample edges may contribute to the signal, while THz generation is local, defined by a laser beam spot (~50 μm in diameter). Finally, we note that in order to generate THz transients in our soft, magnetic Py-based samples with vanishing remanence, an external **H** field was always necessary. On the other hand, our preliminary measurements performed on magnetically harder materials show that after the initial magnetization, no external **H** is required to generate high-intensity THz transients. (Studies of transient THz emission from magnetically harder nanobilayers will be published separately.)

In conclusion, we have generated subpicosecond electromagnetic transients from Ta (2-nm)/Py (2-nm)/Pt (2-nm) spintronic nanotrilayers using a train of 100-fs-wide laser pulses and a static magnetic field (up to ±70 A/m) applied in the plane of a sample. Resulting power spectra of the transients extend up to 5 THz with a 3-dB cutoff at 0.85 THz. The amplitude of the transients depends linearly on the average laser power; however, for the same laser power, blue photons (400-nm wavelength) generate THz

transients with amplitudes approximately 3× larger than transients resulting from excitation by infrared (800-nm-wavelength) photons. The THz amplitude of emitted signals is tunable by the **H**-field intensity and follows the hysteretic behavior of the magnetization versus **H**-field dependence of the pure Py layer, albeit $A^{\mathrm{THz}}(\mathbf{H})$ is, in practice, nonhysteretic. Finally, we note that our simple, robust, and tunable THz emitters can lead to widespread applications in compact, hand-held THz diagnostic devices, in local device-to-device communication with enormous data transfer capacity, or as sources for material and circuit testing at THz frequencies.

The work at the Research Center Jülich was performed within *Ju*SPARC (Jülich Short-pulse Particle Acceleration and Radiation Center), a strategy project funded by the BMBF. Research at Rochester has been supported in part by the grant from the HYPRES Co., and by the New York State Advanced Technology Centers for Innovative and Enabling Technologies (University of Rochester) and Advanced Sensor Technologies (Stony Brook University).

1. M. Tonouchi, Nat. Photonics **1**, 97 (2007); E. A. Williams, *National Association of Broadcasters Engineering Handbook*, 10th ed. (Elsevier, Burlington, MA, 2007).
2. R. A. Lewis, J. Phys. D: Appl. Phys. **47**, 374001 (2014).
3. A. Koroliov *et al*., Appl. Sci. **9**, 391 (2019).
4. K. Ajito and Y. Ueno, IEEE Trans. Terahertz Sci. Technol. **1**, 293 (2011).
5. E. A. Nanni *et al*., Nat. Commun. **6**, 8486 (2015).
6. S. Baierl *et al*., Nat. Photonics **10**, 715 (2016).
7. R. L. Milot *et al*., Nano Lett. **16**, 7001 (2016).
8. G. Torosyan *et al*., Sci. Rep. **8**, 1311 (2018).
9. T. Seifert *et al*., Appl. Phys. Lett. **110**, 252402 (2017).
10. T. Kampfrath *et al*., Nature Nanotechnol. **8**, 256 (2013).
11. Y. Wu *et al*., Adv. Mater. **29**, 1603031 (2017).
12. M. Battiato, K. Carva, and P. M. Oppeneer, Phys. Rev. B **86**, 024404 (2012).
13. D. Rudolf *et al*., Nat. Commun. **3**, 1037 (2012).
14. E. Turgut *et al*., Phys. Rev. Lett. **110**, 197201 (2013).
15. S. Mathias *et al*., Proc. Nat. Acad. Sci. **109**, 4792 (2012).
16. A. Eschenlohr *et al*., Nat. Mater. **12**, 332 (2013).
17. J. Sinova *et al*., Rev. Mod. Phys. **87**, 1213 (2015).
18. G. Li *et al*., J. Phys. D: Appl. Phys. **51**, 134001 (2018).
19. A. Geižutis *et al*., Opt. Mater. **30**, 786 (2008).
20. T. Seifert *et al*., Nat. Photonics **10**, 483 (2016).
21. R. I. Herapath *et al*., Appl. Phys. Lett. **114**, 041107 (2019).
22. E. Saitoh *et al*., Appl. Phys. Lett. **88**, 182509 (2006).